

PART II : HIGH QUALITY SURFACE MESHING USING HARMONIC MAPS

Jean-François Remacle¹ , Christophe Geuzaine², Emilie Marchandise¹

¹ Université catholique de Louvain, Belgium.

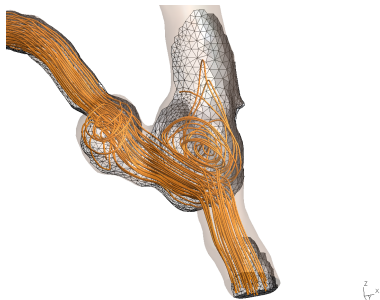
² Université de Liège, Belgium.

<http://www.geuz.org/gmsh>

September 24, 2012

Motivation (1)

Biomedical Engineering: geometries are triangulations

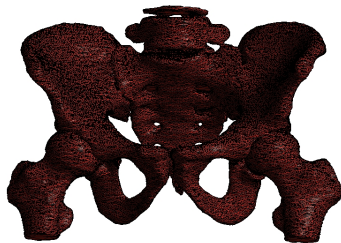


- Numerical simulations require high quality meshes
- Triangulations obtained from imaging techniques are of low quality
 - oversampled
 - non-delaunay triangulations
- Recover high quality surface mesh from low-quality inputs

- Mesh adaptation
Wang 2007, Bechet 2002, ...
- Parametrization of surface
Floater 2005, Sheffer 2006, Marcum 1999, Levy 2004, ...

Motivation (1)

Biomedical Engineering: geometries are triangulations

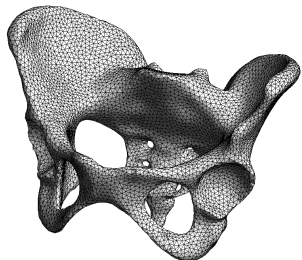


- Numerical simulations require high quality meshes
- Triangulations obtained from imaging techniques are of low quality
 - ① oversampled
 - ② non-delaunay triangulations
- Recover high quality surface mesh from low-quality inputs

- Mesh adaptation
Wang 2007, Bechet 2002, ...
- Parametrization of surface
Floater 2005, Sheffer 2006, Marcum 1999, Levy 2004, ...

Motivation (1)

Biomedical Engineering: geometries are triangulations

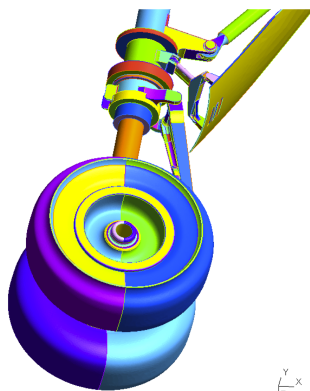


- Numerical simulations require high quality meshes
- Triangulations obtained from imaging techniques are of low quality
 - 1 oversampled
 - 2 non-delaunay triangulations
- Recover high quality surface mesh from low-quality inputs

- Mesh adaptation
Wang 2007, Bechet 2002, ...
- Parametrization of surface
Floater 2005, Sheffer 2006, Marcum 1999, Levy 2004, ...

Motivation (2)

CAD data is not suitable for FE analysis



- Geometric models of a landing gear
- CAD data issued from CATIATM
 - ① 852 surface patches
 - ② we were unable to build a suitable CDF mesh for that model
- Reparametrize through existing patches could be highly useful
 - ① 291 surface patches remaining
 - ② we were able to build a suitable CDF mesh for that model

Motivation (2)

CAD data is not suitable for FE analysis



- Geometric models of a landing gear
- CAD data issued from CATIATM
 - ① 852 surface patches
 - ② we were unable to build a suitable CDF mesh for that model
- Reparametrize through existing patches could be highly useful
 - ① 291 surface patches remaining
 - ② we were able to build a suitable CDF mesh for that model

Outline

- 1 Surface meshing using harmonic maps
- 2 Multiscale partitioning
- 3 Automatic quality meshing
- 4 Quality meshing
- 5 FE Biomedical simulations

Surface parametrization

Parametrizing a surface \mathcal{S} is defining a map $\mathbf{u}(\mathbf{x})$

$$\mathbf{x} \in \mathcal{S} \subset \mathcal{R}^3 \mapsto \mathbf{u}(\mathbf{x}) \in \mathcal{S}^* \subset \mathcal{R}^2 \quad (1)$$

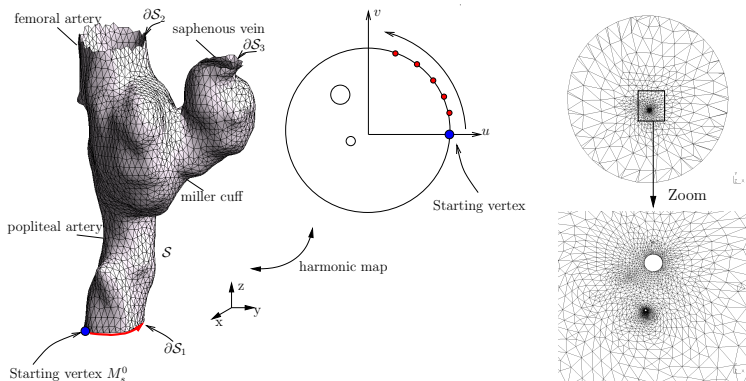


Figure : Mapping an STL triangulation of an arterial anastomosis onto the unit circle and mapped mesh on the unit circle.

Limitations for such a mapping ?

Two topological conditions and one geometrical condition:

- ① Surface of genus $G = 0$
- ② Surface with at least one boundary b
- ③ Aspect ratio $\eta = H/D < 4$

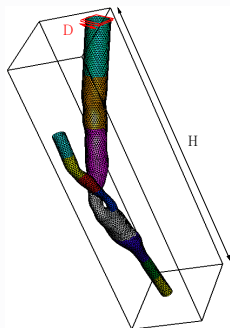
How to compute those conditions ?

The genus G of the surface is computed from the Euler-Poincaré theory:

$$G = \frac{b + \chi(S) - 2}{2}$$

where

- b is the number of boundaries
- $\chi(S)$ is the Euler-Poincaré characteristic of the surface:
- $\chi(S) = \#V - \#E + \#F$



Limitations for such a mapping ?

Two topological conditions and one geometrical condition:

- ① Surface of genus $G = 0$
- ② Surface with at least one boundary b
- ③ Aspect ratio $\eta = H/D < 4$

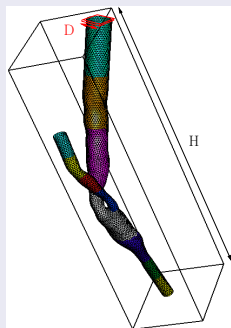
How to compute those conditions ?

The genus G of the surface is computed from the Euler-Poincaré theory:

$$G = \frac{b + \chi(S) - 2}{2}$$

where

- b is the number of boundaries
- $\chi(S)$ is the Euler-Poincaré characteristic of the surface:
- $\chi(S) = \#V - \#E + \#F$



Laplacian harmonic map

To parametrize this surface with harmonic maps, we solve two Laplace equations in the domain \mathcal{S} :

$$\nabla^2 u = 0, \quad \nabla^2 v = 0, \quad \text{on } \mathcal{S} \quad (2)$$

with Dirichlet and Neumann boundary conditions

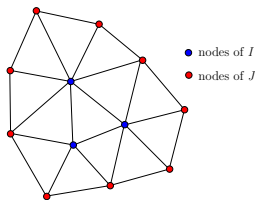
$$u = f_1(\mathbf{x}), \quad v = f_2(\mathbf{x}) \quad \text{on } \partial\mathcal{S}_1, \quad (3)$$

$$\frac{\partial u}{\partial n} = 0, \quad \frac{\partial v}{\partial n} = 0 \quad \text{on } (\partial\mathcal{S} - \partial\mathcal{S}_1). \quad (4)$$

It is easy to prove that eq. (2) and eq. (3)-(4) is equivalent to the following quadratic minimization problem:

$$\min_{\mathbf{u} \in U(\mathcal{S})} J(\mathbf{u}), \quad J(\mathbf{u}) = \frac{1}{2} \int_{\mathcal{S}} |\nabla \mathbf{u}|^2 ds = E_D(\mathbf{u}) \quad (5)$$

Harmonic map with FE's



On the initial mesh, solve the Laplace equations with linear FE's:

$$u_h(\mathbf{x}) = \sum_{i \in I} u_i \phi_i(\mathbf{x}) + \sum_{i \in J} f(\mathbf{x}_i) \phi_i(\mathbf{x}) \quad (6)$$

with appropriate BC's $f_1(\mathbf{x})$, and $f_2(\mathbf{x})$.

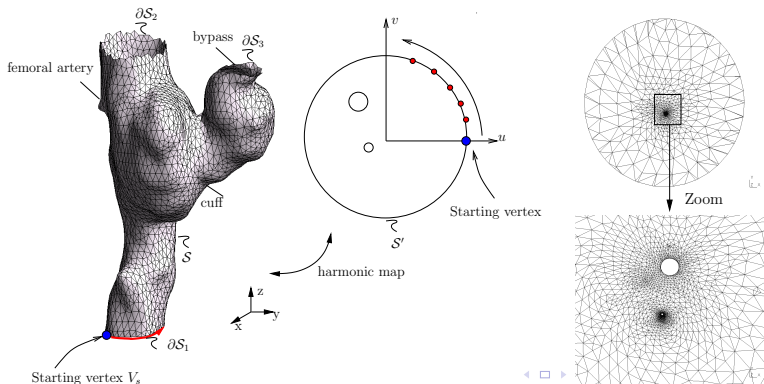
A good choice of functions is given by;

$$u_i = \cos(2\pi l_i/L) \quad , \quad v_i = \sin(2\pi l_i/L), \quad (7)$$

Computing the Mapping using Harmonic Maps

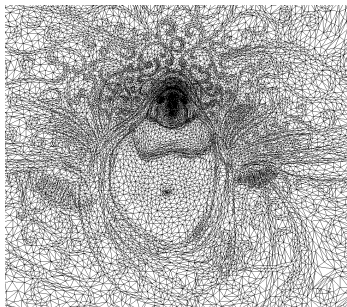
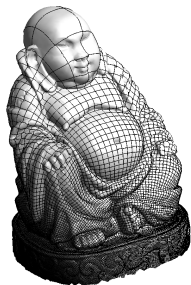
- S is isomorphic to the unit disk.
- We choose a starting vertex arbitrarily, then compute curvilinear abscissa l_i of other nodes on ∂S (length L).
- The position (u_i, v_i) of M_i^0 in the parametric plane can be written as

$$u_i = \cos(2\pi l_i/L) \quad , \quad v_i = \sin(2\pi l_i/L).$$



Computing the Mapping using FE's

- Solve $\nabla^2 u = 0$ on \mathcal{S} with $u = u_i$ as BCs,
- Solve $\nabla^2 v = 0$ on \mathcal{S} with $v = v_i$ as BCs,
- Each internal vertex of the original triangulation has its local coordinates u and v .



Radò-Kneser-Choquet theorem

The harmonic mapping can be proven to be one-to-one, provided that surface S' is convex.

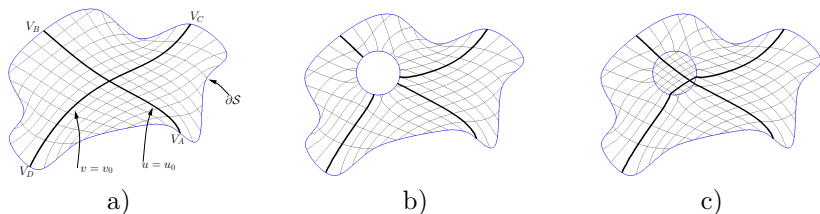


Figure : Iso-values of coordinates u and v on a surface S that are computed as solutions of the Laplace equation on S with boundary conditions that map ∂S on the unit circle. a) Dirichlet boundary conditions are imposed on the outer boundary of S for two configurations: b) S excludes the interior disk and zero Neumann boundary conditions are applied on the inner circular boundary and c) S includes the interior disk, where a small diffusion coefficient is used.

Finite Elements w.r.t. discrete maximum principle.

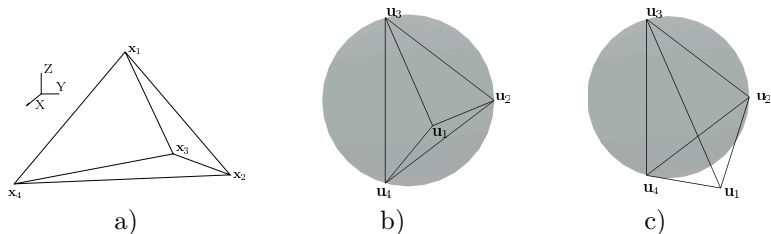
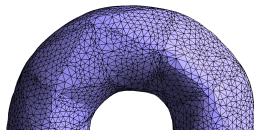
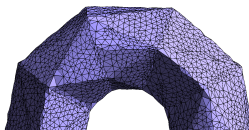
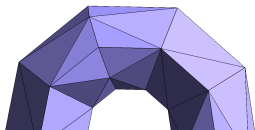
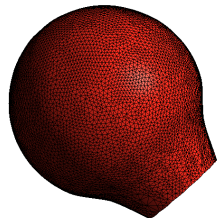
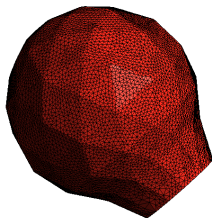
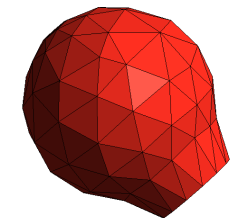


Figure : a) Triangulation for which the discrete harmonic mapping is not guaranteed to be one-to-one: $\mathbf{x}_1 = (r, 0, 1)$ for $r > 0$ and $\mathbf{x}_2 = (1, 1, 0), \mathbf{x}_3 = (0, 0, 0), \mathbf{x}_4 = (1, -1, 0)$. b) Case $r = 1.5$: the mapping is one-to-one, c) Case $r = 3.5$: the mapping is not one-to-one. The point \mathbf{u}_1 does not even lie within the unit disk.

Convex combination maps solves the problem. Other problem: bad parametrization.

Higher order representation of the geometry



Initial STL

Linear map

Cubic map

Outline

- 1 Surface meshing using harmonic maps
- 2 Multiscale partitioning
- 3 Automatic quality meshing
- 4 Quality meshing
- 5 FE Biomedical simulations

Harmonic maps for geometries with large aspect ratio

The issue of undistinguishable coordinates (non uniform flattening of Buddah)



Harmonic maps for geometries with large aspect ratio

The fundamental problem is the PDE

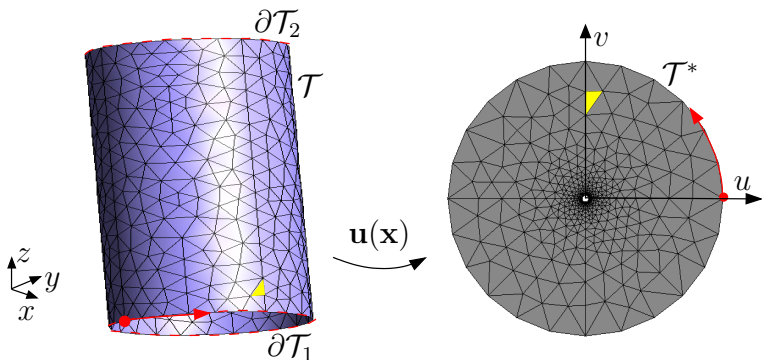
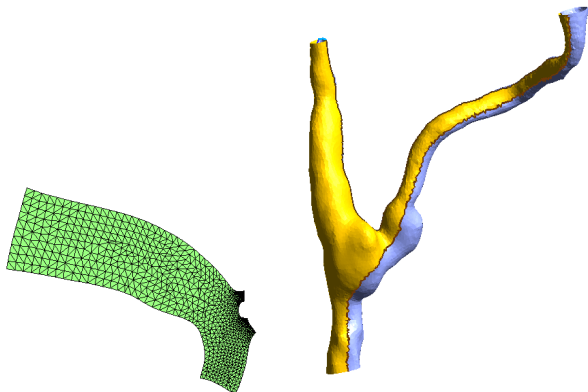


Figure : Parametrization. A piecewise linear map creates a correspondence between a 3D surface mesh M and a 2D mesh M^* of same topology ($G = 0, N_B = 2, \eta = 2$), mapping each triangle from \mathcal{R}^3 to \mathcal{R}^2 .

Max-cut partitioning

Follow idea of alliez et al. [1]: the partition is performed in the parametric space after the computation of a harmonic map.



[1] P. Alliez, M. Meyer, and M. Desbrun. Interactive geometry remeshing. Computer graphics (Proceedings of the SIGGRAPH 02), pages 347–354, 2002.

Harmonic maps for geometries with large aspect ratio

Solution : go multiscale

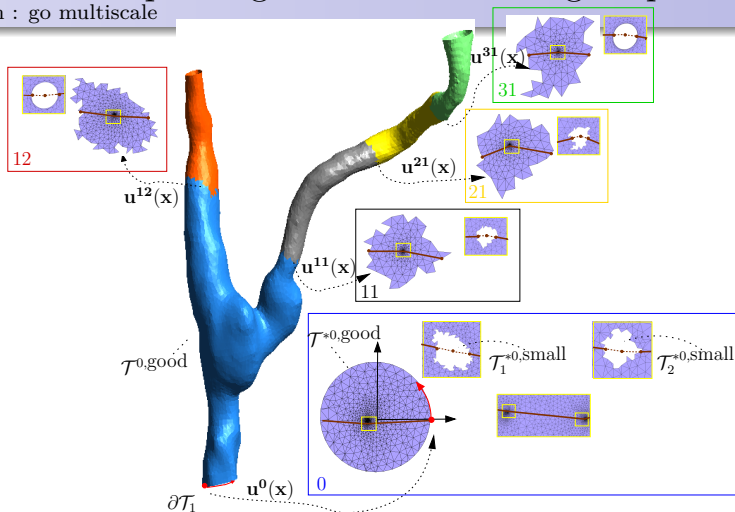


Figure : Multiscale Laplace partitioning method ($G = 0, N_B = 3, \eta = 11$). In this example there are three levels on which a mapping is computed.

Max-cut partitioning based on multiscale Laplace

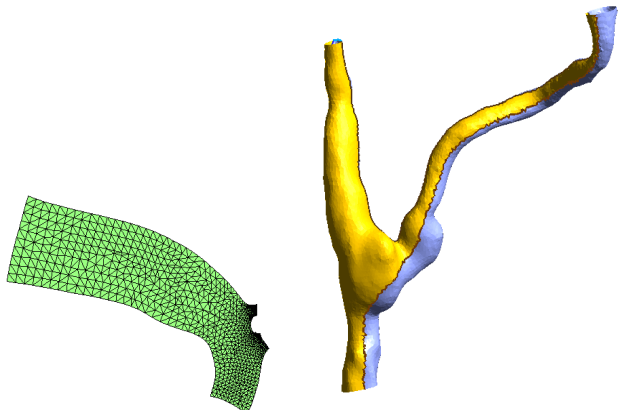


Figure : Multiscale Laplace partitioning method. Initial mesh and partitioned mesh that is appropriate for high precision discrete harmonic mappings .

Partitioning the initial triangulation

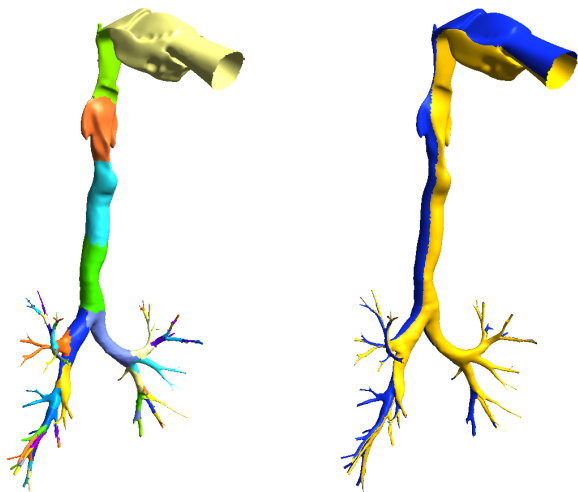
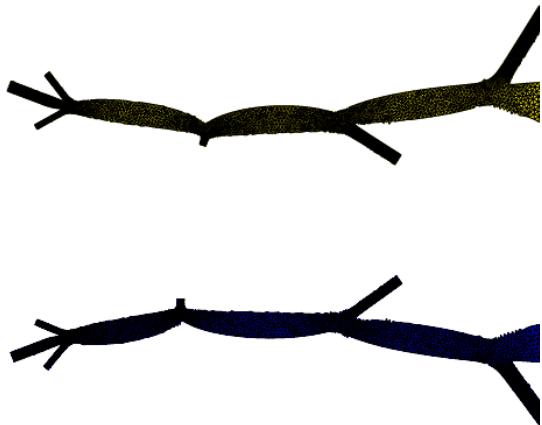
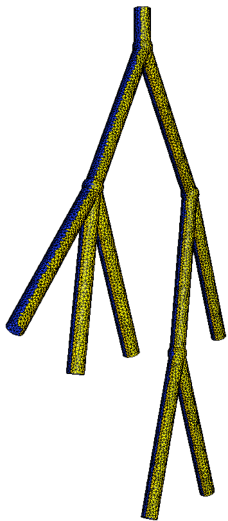


Figure : Partitioning a lung with (left) a recursive multilevel method (Metis) and (right) the multiscale laplacian harmonic partitionner.

Max-cut partitioning based on multiscale Laplace

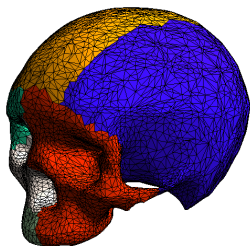
Remeshing of an arterial tree (left) with a conformal map (right).



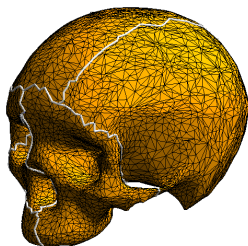
Outline

- 1 Surface meshing using harmonic maps
- 2 Multiscale partitioning
- 3 Automatic quality meshing**
- 4 Quality meshing
- 5 FE Biomedical simulations

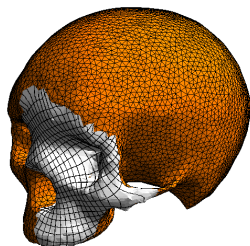
Automatic remeshing



a)



b)

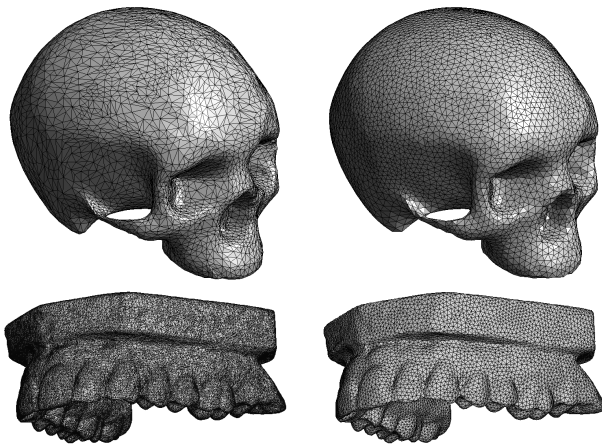


c)

Remeshing algorithm.

- Initial triangulation ($G = 2, N_B = 0$) that is cut into different mesh partitions of zero genus,
- Remesh the lines at the interfaces between partition
- Compute harmonic map for every partition and remesh the partition in the parametric space ($\mathbf{u}(\mathbf{x})$ coordinates visible for one partition).

Automatic remeshing



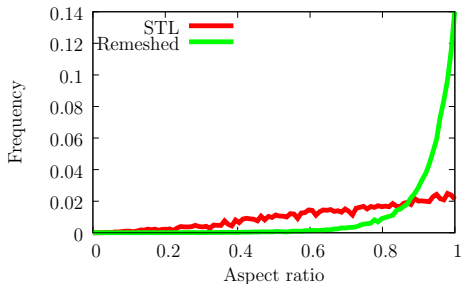
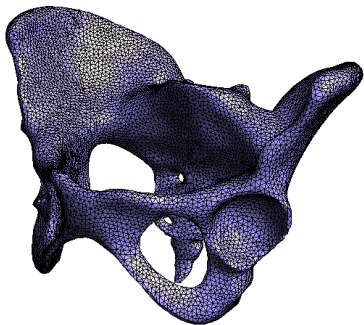
STL triangulations obtained from medical images (Left) that have been automatically remeshed with our automatic remeshing algorithm (Right).

Outline

- 1 Surface meshing using harmonic maps
- 2 Multiscale partitioning
- 3 Automatic quality meshing
- 4 Quality meshing**
- 5 FE Biomedical simulations

High quality meshing

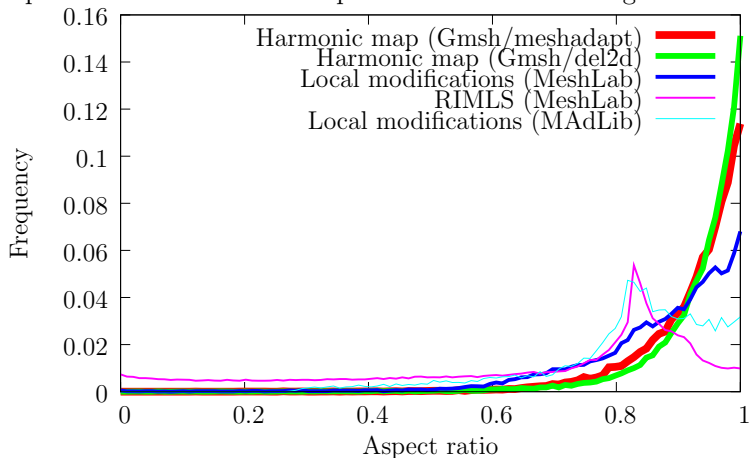
Plot of the quality histogram with high average aspect ratio $\bar{\kappa} = 0.94$:



$$\text{Aspect ratio} = \kappa = 2 \frac{\text{inscribed radius}}{\text{circumscribed radius}} = 4 \frac{\sin \hat{a} \sin \hat{b} \sin \hat{c}}{\sin \hat{a} + \sin \hat{b} + \sin \hat{c}}, \quad (8)$$

High quality meshing

Comparisons with other techniques for surface remeshing:

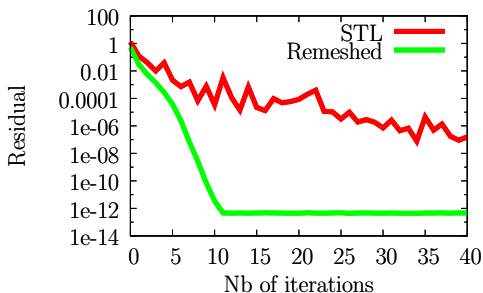
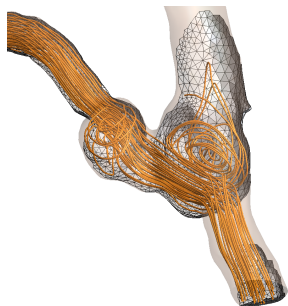


CPU time < 100s for mesh of $1.e^6$ elements

Outline

- 1 Surface meshing using harmonic maps
- 2 Multiscale partitioning
- 3 Automatic quality meshing
- 4 Quality meshing
- 5 FE Biomedical simulations

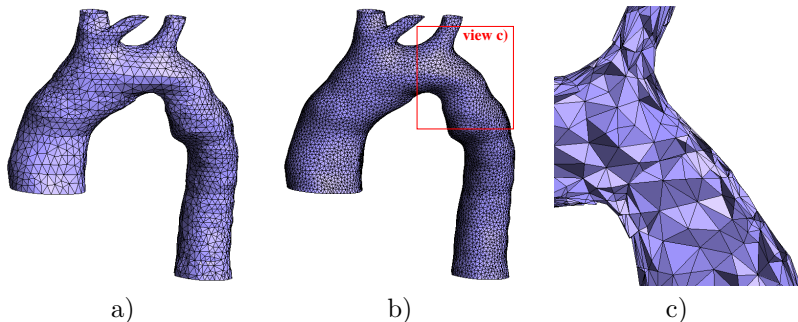
Blood flow in arterial anastomosis



Quality of the surface and volume meshes:

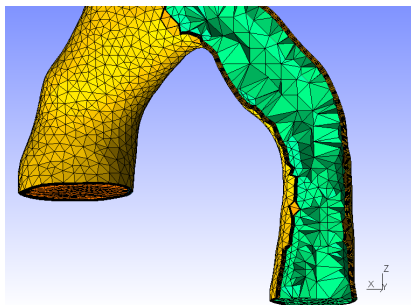
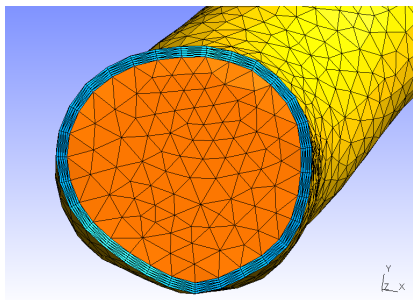
Mesh	Surface quality		Volume quality	
	κ_{min}	$\bar{\kappa}$	γ_{min}	$\bar{\gamma}$
STL	0.0033	0.821	0.0019	0.563
Remeshed	0.6400	0.949	0.2550	0.677

Blood flow in aortic arch



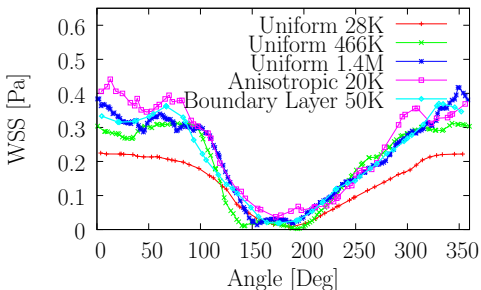
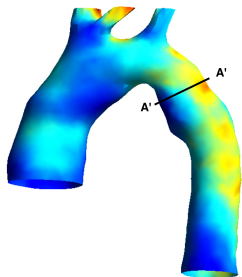
Aortic arch meshes: a) Initial STL triangulation, b) A remeshed surface (isotropic mesh size), c) Volume mesh cut of the anisotropic volume mesh created from the remeshed surface.

Blood flow in aortic arch



Aortic arch meshes: boundary layer meshes.

Blood flow in aortic arch



Blood flow simulation in an aortic arch. The left figure shows the WSS distribution and the right figure the WSS along the circumference at section $A - A'$ for different meshes for a constant inlet flow rate. The zero angle corresponds to the location A' .

Landing Gear

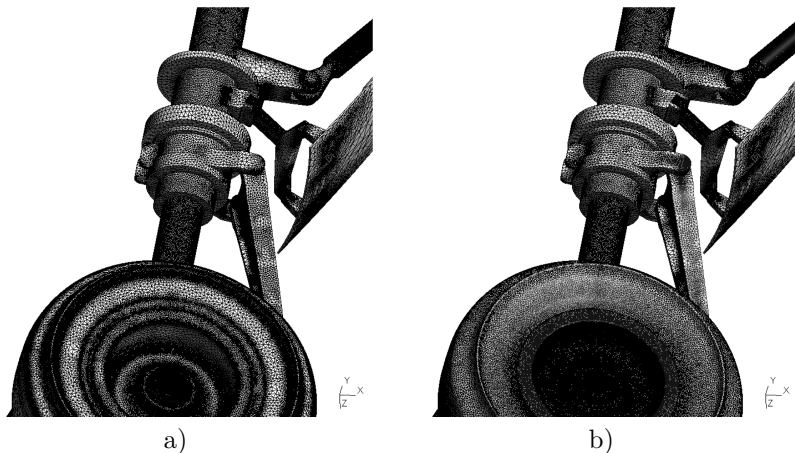


Figure : Remeshing of a landing gear. Left Figure shows the initial mesh with many patches and right Figure shows the mesh with the reparametrized geometry.

Landing Gear

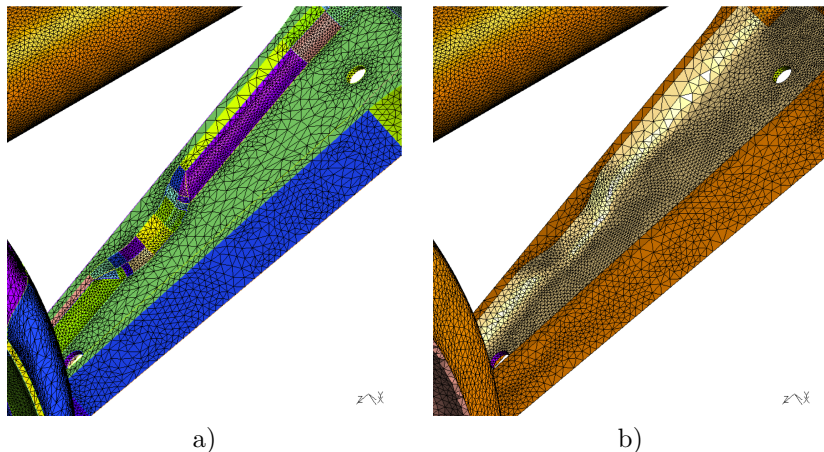


Figure : Remeshing of a landing gear. Left Figure shows the initial mesh with many patches and right Figure shows the mesh with the reparametrized geometry.

Landing Gear



Figure : 3D with Boundary Layer mesh (10 million nodes).

Conclusions

Presented:

- Automatic remeshing STL triangulations
- High quality surface meshes
- Appropriate for FE simulations (2D/3D)

Ongoing work:

- Spectral least square conformal map
- Use conformal maps for generation of quad meshes
- Hexahedral dominant meshes

Thank you for your attention ...

[\[emilie.marchandise, jean-francois.remacle\]@uclouvain.be](mailto:emilie.marchandise, jean-francois.remacle@uclouvain.be)